Combinatorial and topological methods in nonlinear chemical kinetics

Leon Glass*

Institute for Fundamental Studies, Department of Physics and Astronomy, University of Rochester, Rochester, New York 14627

Combinatorial and topological techniques are developed to classify nonlinear chemical reaction networks in terms of their qualitative dynamics. A class of N coupled equations, based on a hypothesis concerning biological control by Monod and Jacob is derived. Transitions between volumes in concentration space for these equations are represented as directed edges on N cubes (hypercubes in N dimensions). A classification of the resulting state transition diagrams for $N = 2,3$ is given. A version of a topological theorem by Poincaré and Hopf is derived which is appropriate for application to chemical systems. This theorem is used to predict the existence of critical points in continuous nonlinear equations with oscillation and bistability on the basis of their state transition diagrams. A large number of nonlinear kinetic equations proposed in previous studies by other authors are classified in terms of their state transition diagrams.

I. INTRODUCTION

Although chemical systems frequently display monotonic decay to equilibrium or steady state, it has been known for over fifty years that chemical systems can also display such exotic behavior as periodic precipitation,[1] homogeneous oscillation,[2] and periodic wave propagation[3] as they evolve in time. Modern interest in these phenomena has been stimulated by a variety of factors, for example, an observation by Turing that reaction diffusion systems can be unstable with respect to periodic spatial concentration perturbations,[4] a conjecture by Monod and Jacob concerning the structure of gene control networks regulating oscillation and differentiation in biological systems,[5] the discovery that oxidation of malonic acid in acid medium (the Belousov–Zhabotinsky reaction) can display rich geometries,[6-8] and the discovery of diverse oscillations of biological origin.[9] A number of excellent reviews have recently appeared which discuss the thermodynamic and kinetic bases of these phenomena.[10-12]

There is a straightforward approach to the study of complex chemical reaction systems. First, determine the equations describing the system, and then solve the equations. However, since there are invariably bimolecular collisions, the equations describing the kinetic systems are nonlinear, and no general methods for finding analytic solutions are known. For example, in studies of the Belousov–Zhabotinsky reaction, complicated kinetics involving a large number of intermediates were found.[13] Further work has lead to a simplification in which there are three nonlinear kinetic equations.[14] The steady states of these equations have been found and a linear stability analysis (see Appendix) carried out in the region of the steady state.[14-16] However, this analysis is cumbersome when only three species are included, and becomes terribly unwieldy if a more complete analysis is attempted.[17] Moreover, a linear stability theory necessarily gives *no* information about the dynamics outside the neighborhood of the critical point. Numerical integration of the Field–Noyes equations has been carried out, but differing time scales can lead to difficulties.[14] We believe that the complications arising in the analysis of the Belousov–Zhabotin-

sky reaction are typical of what will be found when chemical systems displaying rich kinetics are analyzed in greater detail. Here, we attempt to bypass many of these difficulties by making maximal use to combinatorial and topological techniques to classify nonlinear dynamics in a class of equations representing model chemical networks. This approach is similar to the application of group theoretical and topological techniques in studies of lattice vibrations in solids.[18-21] We stress at the outset that the analysis and classification in no sense obviates the need for a complete study of realistic kinetic equations. It is meant to provide a conceptual base from which a more detailed analysis can be mounted.

This work has arisen from an attempt to unify two apparently disparate theoretical approaches.

(1) In an analysis of the Field–Noyes equations it was shown that all trajectories enter a volume in concentration space, the eight boxes in Fig. 1(a).[15] Further, all trajectories in Boxes 5 and 4 (except for a singular trajectory in each box) leave them and eventually cycle through the remaining six boxes in the sequence[22]

$$B3 \rightarrow B1 \rightarrow B2 \rightarrow B6 \rightarrow B8 \rightarrow B7 \rightarrow B3 \rightarrow \cdots$$

If we define the Boolean variables

$$\tilde{x}_i = 1 \text{ if } x_i \geq \theta$$
$$\tilde{x}_i = 0 \text{ if } x_i < \theta \ , \tag{1}$$

where the concentrations θ_i are given by the vertex common to all eight boxes, the transitions between volumes in concentration space can be mapped on the edges of a cube, as in Fig. 1(b). The representation in Fig. 1(b) is called a *state transition diagram*.

(2) Several authors have argued that biological control networks bear strong similarities to discrete switching networks.[23-26] In studies of the dynamics of nonlinear networks, it was found by numerically integrating the nonlinear equations that there was a strong connection between the logical structure of an underlying switching network, and transitions in a discrete phase space.[25] More recently, it was shown how the state transition diagrams for a discrete system can be embedded on a cube, as in Fig. 1(b), and a classifica-

tion of the resulting state transition diagrams in two and three dimensions was given.[27]

In the following we show how the transitions between volumes in concentration space can be related to an underlying logical network, and show how restrictions on these transitions can be predicted once the structure of the underlying network is known. Our emphasis on classification of the dynamics is similar to recent studies in which the critical points of dynamical equations representing chemical[16] or ecological[28,29] systems have been classified on the basis of the signs of the linearized equations of motion in the region of the critical point (Appendix). However, by considering the topological properties of chemical concentration space, the number and types of critical points in different parts of phase space can be related to one another, and a better picture of the global dynamics can be achieved.

In Sec. II we derive nonlinear kinetic equations for N chemical species and show how the state transition diagrams for the equations when the discretization in Eq. (1) is performed can be embedded on an N-cube (hypercube in N dimensions). In Sec. III, we classify the state transition diagrams into equivalence classes using combinatorial and topological arguments. A type of critical point, called the extremal steady states here, can be predicted from the state transition diagrams. However, in order to be consistent with topological re-

quirements, it is often necessary that additional critical points be present in the concentration space. The minimum number and types of these critical points are given in Sec. IV. In Sec. V, we illustrate these methods by showing the connection between the abstract results and nonlinear dynamics in two systems of biological and chemical interest. A number of kinetic schemes proposed in earlier work are classified into one of these systems. The results are discussed in Sec. VI. In the Appendix we review the topological index theorems used in Secs. III and IV.

II. STATE TRANSITION DIAGRAMS FOR NONLINEAR KINETIC EQUATIONS

Jacob and Monod discovered the genetic mechanisms by which the synthesis of the enzyme galactosidase in the bacteria $E.coli$ is regulated by the concentration of its substrate, lactose.[30] Subsequent studies have shown that the dependence of synthetic rate on lactose concentration is roughly described by the Hill function[31]

$$f_H = \frac{\lambda x^n}{\theta^n + x^n} \quad , \tag{2}$$

where λ is a production constant, θ is a "threshold," and n is a parameter which is approximately 2 for the lactose–galactosidase system. On the basis of their studies, Monod and Jacob hypothesized that cellular dynamics might be controlled by networks in which the products from one enzyme serve to regulate the synthesis of other enzymes in the cell.[5] Although this hypothesis has not been either confirmed or repudiated, it has stimulated a large body of theoretical work[32-38] in which authors have studied the qualitative properties of reaction networks described by the equations

$$\frac{dx_i}{dt} = \lambda_i f_i(x_1 x_2 \cdots x_{i-1} x_{i+1} \cdots x_N) - \gamma_i x_i, \quad i = 1, N \tag{3}$$

where f_i describes the kinetics of synthesis of the ith compound and λ_i and γ_i are production and decay constants, respectively, for this compound.

Here, we show how the qualitative dynamics of Eq. (3) can be determined and classified for a particularly severe set of restriction on the f_i. These restrictions can be simply stated. For each of the N variables in Eq. (3) we associate a Boolean variable $\tilde{x}_i$ defined in Eq. (1) where we further require $\lambda_i/\gamma_i > \theta_i$. We then assume that f_i is a Boolean function B_i so that the resulting network can be written

$$\frac{dx_i}{dt} = \lambda_i B_i(\tilde{x}_1 \tilde{x}_2 \cdots \tilde{x}_{i-1} \tilde{x}_{i+1} \cdots \tilde{x}_N) - \gamma_i x_i \quad i = 1, \quad i = 1, \ N. \tag{4}$$

If there are N variables, there are 2^N Boolean states. A Boolean function assigns a value of 1 or 0 to each of these states. Therefore there is a choice of $2^{2^{N-1}}$ functions for each B_i and there are potentially $2^{N \times 2^{N-1}}$ different networks of the form in Eq. (4).

We have given numerical evidence that the qualitative dynamics of many equations based on Eq. (3) are invariant to a wide range of parametric changes in f_i and remain unchanged even when the f_i are discontinuous as in Eq. (4).[37,39,40] Further, as we shall see later, the
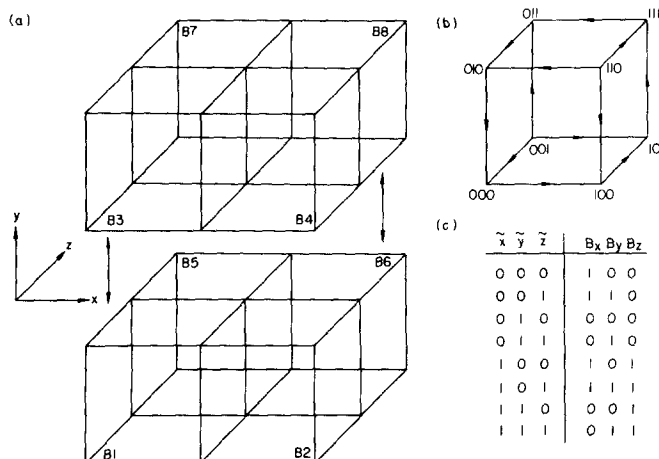

FIG. 1. (a) A decomposition of a volume of concentration space of the Field–Noyes equations[14] given by Hastings and Murray.[15,22] To aid presentation, the volume has been separated into upper and lower halves, but these are contiguous. The variables x, y, z are associated with the chemicals $HBrO_2$, Br^-, and Ce^{IV}, respectively. All trajectories enter the volume of concentration space shown. All trajectories in Boxes 5 and 4 (except for a singular trajectory in each box) leave these volumes and enter into volumes $B1$, $B7$, $B6$ or $B3$, $B8$, $B2$, respectively. All trajectories not in $B5$ and $B4$ cycle through the sequence $B3 \rightarrow B1 \rightarrow B2 \rightarrow B6 \rightarrow B8 \rightarrow B7 \rightarrow B3 \rightarrow \cdots$. The vertex common to all eight boxes is an unstably steady state of the Field–Noyes equations. (b) The state transition diagram giving the transitions described in Fig. 1(a), when Eq. (1) is applied. Each vertex represents one of the eight boxes of concentration space shown in Fig. 1(a). (c) The Boolean functions which when substituted in Eq. (4) generate the state transition diagrams in Fig. 1(b). Given either Fig. 1(b) or 1(c) the other can be genrated unambiguously using the techniques described in Sec. II. A verbal description of the interactions in Fig. 1(c) is: x activates z, z activates y, y inhibits x. (cf. Ref. 16).

qualitative dynamics of many nonlinear chemical systems which have been proposed to date fit neatly into the classification scheme which we find for Eq. (4).

Equation (4) displays sharp restrictions on the transitions between the Boolean states found using Eq. (1).[41] The nature of these restrictions can be easily determined. Assume that at some time t, $x_i < \theta_i$. If $B_i = 0$, $\dot{x}_i < 0$ and x_i will remain smaller than θ_i. Unless B_i changes, x_i will be constrained to remain smaller than θ_i. In contrast, if $B_i = 1$, $\dot{x}_i > 0$, and it is possible that at some future time, x_i can cross its threshold. In a similar way, if x_i is initially greater than θ_i it can only pass through its threshold if $B_i = 0$.

A graphical representation of these restrictions is provided by embedding the allowable transitions on a Boolean N-cube.[27,42] On a Boolean N-cube there are 2^N vertices and $N \times 2^{N-1}$ edges. The vertices can be labeled by a Boolean state so that each vertex is connected to the N vertices which differ from it in one locus. Transitions which are allowed by the B_i are indicated by drawing a directed arrow from the first state to all allowed states. We exclude transitions in which more than one variable changes simultaneously, so that each allowable transition can be represented by a directed edge on the N-cube. The restriction of no self-input on the B_i requires that each edge on the N-cube have an arrow in one and only one orientation. In Fig. 1(c) we give the Boolean functions which generate the state transition diagram in Fig. 1(b).

Each network gives a unique assignment of orientations to the edges of the Boolean N-cube. As we have noted there are $2^{N \times 2^{N-1}}$ different networks for N-chemical species, or 16 networks for $N = 2$, 4096 networks for $N = 3$, and 2^{32} networks for $N = 4$. Two networks will be said to be in the same *structural equivalence class* if their state transition diagrams can be identically superimposed under some symmetry operation of the N-cube. By using the Polya enumeration theorem it is possible to determine the number of structural equivalence classes from the symmetry group of the N-cube. We have shown that the number of structural equivalence classes is 4 for $N = 2$ and 112 for $N = 3$.[27] The four equivalence classes for $N = 2$ are shown in Fig. 2. A
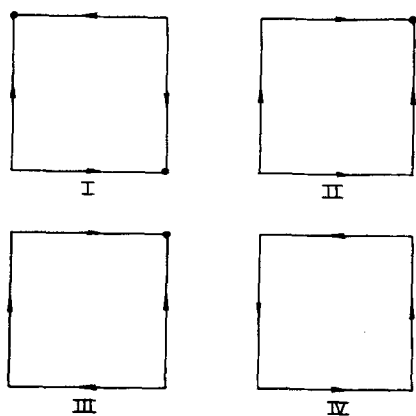
vertex which only has arrows entering (leaving) it will be called an (un)*stable node* and a continuous path which comes back on itself will be called a *cycle*. For example, in Fig. 1(b) there are two unstable nodes and one cycle. If the stable nodes and cycles of two networks can be superimposed under some symmetry operation of the N-cube, they will be said to be *dynamically equivalent*. We have shown that there are 13 dynamical equivalence classes for $N = 3$ for systems with at least a single stable node.[27] In the following section we use topological properties of the directed graphs on the cube to give a finer enumeration of the equivalence classes for $N = 3$.

III. EQUIVALENCE CLASSES OF NONLINEAR KINETIC EQUATIONS

By embedding the directed graph on the skeleton of the cube on the surface of the sphere, we can apply a combinatorial version of the topological index theorems (Appendix).[43,44] For this case the theorem states

$$\vcenter{\hbox{\includegraphics}} + \vcenter{\hbox{\includegraphics}} + \vcenter{\hbox{\includegraphics}} - \vcenter{\hbox{\includegraphics}} = 2 \ , \quad (5)$$

where each diagram in Eq. (5) represents the number of times each configuration appears on the state transition diagram. (This relationship is a direct consequence of the familiar Euler theorem for simple polyhedra, $F - E + V = 2$, where F, E, V are the numbers of faces, edges, and vertices, respectively, of a polyhedron).

Two dynamical systems given in Eq. (4) will be considered to be in the same *surface equivalence class* if all the configurations in Eq. (5) in one state transition diagram can be superimposed identically on the same configurations of the other system under some symmetry operation of the cube. We enumerate all the surface equivalence classes for Eq. (4) with $N = 3$. The combinatorial techniques to do this are well established and will only be briefly given.[27,42,44,45]

Starting with the system with four stable nodes we generate in turn the various surface equivalence classes. The location of stable and unstable nodes for each structure is indicated in Table I by giving the vertex where each configuration appears. The faces on which cycles and saddles appear is specified by giving the one Boolean variable which is constant on a face with xs in the other two loci (as in $0xx$). Several of the structures have saddles and cycles on identical faces but the loci of the stable and unstable nodes are interchanged. For these structures, one of the structures is indicated by a prime in Table I. In addition, we compute the number of dynamical systems C_i (out of 4096) that are in each surface equivalence class. C_i is computed as follows. Given the location of the configuration in Table I and the fact that *no* other configurations in Eq. (5) can appear in the state transition diagrams, we generate the state diagram for each equivalence class. Each of the 48 symmetry elements of the cube will leave a state transition diagram invariant or map it to another orientation on the cube. The number of

FIG. 2. The four structural equivalence classes for $N = 2$. The number of systems in each class is 2, 4, 8, 2, respectively.

TABLE I. A listing of the surface equivalence classes for $N=3$. Each structure is listed at the left followed in parentheses by the number of structural equivalence classes for the structure where this number is different from 1. For each structure, the vertex or face on which the four symbols in Eq. (5) are located are given. On the basis of this information, and the fact that the structures in Eq. (5) are found in no other loci besides those listed, state transition diagrams of the sort shown in Fig. 1b can be constructed. The remaining columns summarize the computations which were performed to determine C_i the number of networks (out of 4096) falling in each surface equivalence class, as described in the text. In structures XLI and XLII, the cycles on opposite faces are in the same and opposite orientations, respectively. One orientation of structure XII' is shown in Fig. 1 (b). The 13 dynamical equivalence classes for structures having at least a single steady state are given in Ref. 27.

Structure					Γ_i	P_i	$j-P_{ij}$	D_i	C_i
I	001,010,100,111	000,011,101,110	• • •	$0xx,1xx,x0x$ $x1x,xx0,xx1$	2	1	• • •	1	2
II	001,010,111	000,011,101	• • •	$0xx,x0x,x1x$ $xx1$	24	1	• • •	1	24
III	001,010,111	011,100	• • •	$0xx,x1x,xx1$	8	1	• • •	1	8
IV	001,010,111	000,011	• • •	$0xx,x1x,xx1$	24	1	• • •	1	24
III'	011,100	001,010,111	• • •	$0xx,x1x,xx1$	8	1	• • •	1	8
V	011,100	010,101	• • •	$0xx,1xx$	24	1	• • •	1	24
VI	011,100	010,101	• • •	$1xx,x0x$	24	1	• • •	1	24
VII	011,100	010,111	• • •	$x0x,x1x$	24	1	• • •	1	24
VIII	011,100	010,111	• • •	$x1x,xx1$	48	1	• • •	1	48
IX	011,100	110	• • •	$1xx$	48	1	• • •	1	48
X	011,100	110	• • •	$x0x$	24	1	• • •	1	24
XI	011,100	110	• • •	$0xx$	48	1	• • •	1	48
XII	011,100	• • •	• • •	• • •	8	1	• • •	1	8
IV'	010,111	000,011,110	• • •	$0xx,x1x,xx0$	24	1	• • •	1	24
VII'	010,111	011,100	• • •	$x0x,x1x$	24	1	• • •	1	24
VIII'	010,111	011,100	• • •	$x1x,xx1$	48	1	• • •	1	48
XIII	010,111	000,101	• • •	$x0x,x1x$	12	1	• • •	1	12
XIV	010,111	001,100	• • •	$x0x,x1x$	12	1	• • •	1	12
XV	010,111	011,110	• • •	$x0x,x1x$	12	1	• • •	1	12
XVI	010,111	011,110	• • •	$1xx,x1x$	48	1	• • •	1	48
XVII(2)	010,111	000,011	• • •	$0xx,x1x$	48	2	• • •	2	96
XVIII	010,111	011,110	$x0x$	$0xx,1xx,x1x$	24	1	• • •	1	24
XIX	010,111	011	$x0x$	$0xx,x1x$	48	1	• • •	1	48
XX	010,111	• • •	$x0x$	$x1x$	24	1	• • •	1	24
XXI(2)	010,111	011	• • •	$x1x$	24	4	VII'-1	3	72
XXII(2)	010,111	000	• • •	$x1x$	24	4	XIII-1	3	72
XXIII(2)	010,111	100	• • •	$x1x$	24	4	XIV-1	3	72
IX'	010	011,100	• • •	$0xx$	48	1	• • •	1	48
X'	010	011,100	• • •	$xx1$	24	1	• • •	1	24
XI'	010	011,100	• • •	$x0x$	48	1	• • •	1	48
XIX'	010	011,110	$x0x$	$0xx,x1x$	48	1	• • •	1	48
XXI'(2)	010	011,110	• • •	$x1x$	24	4	VII-1	3	72
XXII'(2)	010	101,110	• • •	$1xx$	24	4	XIII-1	3	72
XXIII'(2)	010	100,111	• • •	$1xx$	24	4	XIV-1	3	72
XXIV	010	011	$1xx,x0x$	$xx0,xx1$	24	1	• • •	1	24
XXV	010	011	$1xx,x0x$	$0xx,x1x$	24	1	• • •	1	24
XXVI	010	• • •	$1xx,x0x$	$xx1$	24	1	• • •	1	24
XXVII	010	• • •	$1xx,x0x$	$0xx$	48	1	• • •	1	48
XXVIII(2)	010	• • •	$1xx,x0x$	$xx0$	24	4	XXIV-1	3	72
XXIX(4)	010	011	$x0x$	$0xx$	48	4	• • •	4	192
XXX	010	011	$x0x$	$xx0$	48	1	• • •	1	48
XXX'	010	011	$x0x$	$xx1$	48	1	• • •	1	48
XXXI	010	011	$x0x$	$x1x$	48	1	• • •	1	48
XXXII	010	011	$x0x$	$1xx$	48	1	• • •	1	48
XXXIII(2)	010	111	$x0x$	$1xx$	48	2	• • •	2	96
XXXIII'(2)	010	111	$x0x$	$xx0$	48	2	• • •	2	96
XXXIV(7)	010	• • •	$x0x$	• • •	48	16	XIX-1 XX-1 XXVI-1 XXVII-1 XXX'-1 XXXI-1 XXXII-1 XXXIII'-1	7	336
XXXV(6)	010	011	• • •	• • •	24	32	VI-1 X-3	11	264

TABLE I (*Continued*).

Structure					Γ_i	P_i	$j - P_{ij}$	D_i	C_i
XXXVI(8)	010	111	•••	•••	24	64	X'-3 XIII-1 XXI-3 XXI'-3 XXIV-1 XXX-2 XXX'-2 XXXII-2 III-1 III'-1 V-2 VI-2 VII-2 VII'-2 VIII-4 VIII'-4 IX-2 IX'-2 X-1 X'-1 XI-2 XI'-2 XIV-2 XXIII-6 XXIII'-6 XXXIII-4 XXXIII'-4	14	336
XXXVII(5)	010	101	•••	•••	8	64	I-1 II-6 IV-3 IV'-3 XIII-3 XVII-12 XXII-9 XXII'-9	18	144
XII'	•••	010, 101	•••	•••	8	1	•••	1	8
XX'	•••	010, 111	$x0x$	$x1x$	24	1	•••	1	24
XXVI'	•••	010	$1xx, x0x$	$xx1$	24	1	•••	1	24
XXVII'	•••	010	$1xx, x0x$	$0xx$	48	1	•••	1	48
XXVIII'(2)	•••	010	$1xx, x0x$	$xx0$	24	4	XXIV-1	3	72
XXXIV'(7)	•••	010	$x0x$	•••	48	16	XIX'-1 XX'-1 XXVI'-1 XXVII'-1 XXX-1 XXXI-1 XXXII-1 XXXIII-2	7	336
XXXVIII	•••	•••	$0xx, 1xx, xx0$ $xx1$	$x0x, x1x$	6	1	•••	1	6
XXXIX	•••	•••	$1xx, xx0, xx1$	$x1x$	24	1	•••	1	24
XL	•••	•••	$1xx, xx0, xx1$	$x1x$	48	1	•••	1	48
XLI(4)	•••	•••	$xx0, xx1$	•••	6	16	•••	16	96
XLII	•••	•••	$xx0, xx1$	•••	6	16	XXXVIII-2 XXXIX-12	2	12
XLIII(6)	•••	•••	$1xx, xx0$	•••	24	32	XXIV-1 XXV-1 XXVI-1 XXVI'-1 XXVII-2 XXVII'-2 XXVIII-3 XXVIII'-3 XXXVIII-1 XXXIX-2 XL-4	11	264

orientations Γ_i in which the ith equivalence class can appear is given by

$$\Gamma_i = 48/h_i \quad , \tag{6}$$

where h_i is the number of elements of the group which leave any member of the ith equivalence class invariant. Although in most cases the specification of the relative locations of the configurations in Eq. (5) specify the orientations of all edges in the cube, this is not always the case. If there are m_i edges left unspecified, then there are

$$P_i = 2^{m_i} \tag{7}$$

permutations of the remaining edges for each orientation of the state transition diagram. However, if P_{ij} of these permutations fall in the jth equivalence class, the number of net permutations falling in the ith class D_i is

$$D_i = P_i - \sum_j P_{ij} \quad . \tag{8}$$

C_i is then computed,

$$C_i = \Gamma_i \times D_i \quad . \tag{9}$$

The computations are summarized in Table I. For completeness we give in parentheses following each structure the number of structural equivalence classes (out of 112) in each surface equivalence class if this number is different from 1.

In Table I, there are 2 structures with 4 stable nodes; 56 structures with 3 stable nodes; 844 structures with 2 stable nodes; 2232 structures with 1 stable node, and 962 structures with no stable nodes. This agrees with previous computations.[27] In addition, the total number of structural equivalence classes is computed to be 112, as it should be. In the following section we consider some of the information about the qualitative dynamics of Eq. (4) which can be found from the state transition diagrams.

IV. CONSTRUCTION OF THE MINIMAL SET OF CRITICAL POINTS FROM THE STATE TRANSITION DIAGRAMS

The state transition diagrams give information about flows between the volumes of concentration space for the dynamical systems in Eq. (4). If there are one or more arrows leaving a vertex, then for any initial point in the volume, there will pass a trajectory which must cross the threshold of one of the variables. Therefore, there can be no steady states in any volume represented by a vertex which has one or more arrows directed away from it. A different situation arises for stable nodes, which only have arrows directed toward the vertex. From the construction given in Sec. II, a stable node will be present for any set of states $\bar{x}_i$, such that

$$\bar{x}_i = B_i \, , \quad i = 1, N \quad . \tag{10}$$

No trajectories starting in the volume designated by the stable node ever leaves this volume. By integrating Eq. (4), we see that in the limit $t \to \infty$, the concentration for each variable in Eq. (4) will be given

$$x_i = (\lambda_i / \gamma_i) B_i \, , \quad i = 1, N \quad . \tag{11}$$

The set of values in Eq. (11) are a steady state of Eq. (4) for any vertex at which Eq. (10) is satisfied. If Eq. (4) is linearized at the steady state of Eq. (11) (see Appendix), the off diagonal elements of the stability matrix will be zero, and the diagonal elements will be the set $-\gamma_i$. Therefore, all the eigenvalues of the stability matrix are negative, and the steady state in Eq. (11) is stable. The steady states satisfying Eq. (10) will be called *extremal steady states*. There are no steady states in Eq. (4) corresponding to unstable nodes in the state transition diagrams.

In the Appendix we give a version of the Poincaré–Hopf theorem appropriate for application to chemical kinetic systems. The theorem can be written

$$\sum_i (-1)^{r_i} = 1 \quad , \tag{12}$$

where π_i is the number of positive eigenvalues of the ith critical point and the sum is over all critical points of the system. The theorem is only for systems in which there are only isolated hyperbolic critical points (see Appendix). The systems defined in Eq. (4) are discontinuous and therefore physically unrealistic around the threshold axes $x_i = \theta_i$. Outside of this region, behavior is smooth and the only critical points which are found are the extremal steady states. We assume without proof that continuous analogues of the discontinuous Boolean functions can be found such that when they are substituted in Eq. (4), behavior will physically realistic (mathematically generic) and isolated hyperbolic critical points will be generated in the region of the threshold axes without generating additional critical points in the remainder of concentration space. For this new continuous system, mathematically and physically "close" to Eq. (4), the Poincaré–Hopf theorem can be applied. Say there are s extremal steady states. Since each extremal steady state is stable and has zero positive eigenvalues, from Eq. (12) we find

$$\sum (-1)^{r_i} = 1 - s \quad , \tag{13}$$

where the sum is restricted to the set of new critical points generated in the neighborhood of the threshold axes by the smoothing operation. For $s \neq 1$, the only way for Eq. (13) to be satisfied is for additional critical points to be generated by the smoothing operation. Calling ϵ the number of additional critical points with an even number of positive eigenvalues, and ω the number of additional critical points with an odd number of positive eigenvalues, we find

$$\epsilon - \omega = 1 - s \quad . \tag{14}$$

The *minimal set* of critical points is that set for which ϵ and ω assume their lowest values. For example, if $s = 0$, the minimal set is given by $\epsilon = 1$, $\omega = 0$; if $s = 2$, the minimal set is given by $\epsilon = 0$, $\omega = 1$.

The results in this section depend on the existence of smooth functions analogous to the discontinuous Boolean functions. The Boolean switching function on one variable is called the Heaviside function. A smooth analogue

of this function is the Hill function, Eq. (2), where n assumes some appropriately large value. In the following section we consider the additional critical points which are generated when Eq. (2) is substituted for the Heaviside function in systems of chemical interest.

V. CRITICAL POINTS FOR CHEMICAL SYSTEMS WHICH DISPLAY OSCILLATION AND BISTABILITY

In Fig. 2 and Table I we give a census of possibilities for the dynamics which are found for Eq. (4) for $N = 2, 3$. Here we show how the state transition diagrams for two chemically and biologically important reaction networks can be computed on the basis of a qualitative description of interactions between the reactants. From the state transition diagrams it is then possible to make predictions concerning the minimal set of critical points for each reaction network. We then determine the critical points of a continuous nonlinear differential equation of the form in Eq. (3), and show how the critical points correspond to the minimal set predicted on the basis of the state transition diagrams.

In feedback inhibition, the last substance in a reaction chain inhibits the production of the first substance. A schematic representation of feedback inhibition can be given by

$$\overline{x_1 \pm x_2 \pm \cdots x_i \pm \cdots x_N} \quad . \tag{15}$$

Networks of this sort often display oscillation.[5,16,23,25,32,33,35-40,46] If there are two consecutive inhibitory steps in a cyclic reaction chain, the network can be represented

$$\overline{x_1 \doteq x_2 \pm \cdots x_i \pm \cdots x_N} \quad . \tag{16}$$

Networks of this sort often display bistability.[5,16,23,25,34,37-39,46]

A network in Eq. (4) can be constructed for each of these schemes by identifying the interaction $x_i \pm x_{i+1}$ with the Boolean function

$\tilde{x}_i$	B_{i+1}
1	1
0	0

$$\tag{17}$$

and the interaction $x_i \doteq x_{i+1}$ with the Boolean function

$\tilde{x}_i$	B_{i+1}
1	0
0	1

$$\tag{18}$$

Using the techniques described in Sec. II, the state transition diagrams for Eqs. (15) and (16) can be computed. For Eq. (15), the state transition diagram is given in Fig. 2, structure IV for $N = 2$, and Table I, structure XII' [(Fig. 1(b)] for $N = 3$. For Eq. (16), the state transition diagram is given in Fig. 2, structure I for $N = 2$, and Table I, structure XII for $N = 3$. For Eq. (15), there are no stable nodes in the state transition diagram, $s = 0$ in Eq. (14), and in the minimal set of critical points there is at least one critical point with an even number of positive real parts. For Eq. (16), there are two stable nodes in the state transition diagram, so there must

be at least one additional critical point with an odd number of positive real parts.

We can now construct the continuous nonlinear differential equations of Eq. (3) by using Hill functions to represent the interactions given in Eqs. (15) and (16). For the interaction $x_i \pm x_{i+1}$ we substitute

$$f_{i+1} = \frac{x_i^n}{\theta_i^n + x_i^n} \, , \tag{19}$$

and for the interaction $x_i \doteq x_{i+1}$ we substitute

$$f_{i+1} = \frac{\theta_i^n}{\theta_i^n + x_i^n} \quad . \tag{20}$$

In the limit $n \to \infty$, Eqs. (19) and (20) correspond to the Boolean functions given in Eqs. (17) and (18), respectively. To simplify computations we assume $\lambda_i = \gamma_i = 1$, $\theta_i = 0.5$ for all i.

The network corresponding to Eq. (15) is then,

$$\frac{dx_1}{dt} = \frac{0.5^n}{x_N^n + 0.5^n} - x_1 \, ,$$

$$\frac{dx_i}{dt} = \frac{x_{i-1}^n}{x_{i-1}^n + 0.5^n} - x_i \, , \quad 2 \le i \le N \, . \tag{21}$$

Corresponding to Eq. (16), we have

$$\frac{dx_1}{dt} = \frac{0.5^n}{x_N^n + 0.5^n} - x_1 \, ,$$

$$\frac{dx_2}{dt} = \frac{0.5^n}{x_1^n + 0.5^n} - x_2 \, , \tag{22}$$

$$\frac{dx_i}{dt} = \frac{x_{i-1}^n}{x_{i-1}^n + 0.5^n} - x_i \, , \quad 3 \le i \le N \, ,$$

where the third equation is needed if $N \ge 3$. By inspection we see that there is a critical point at $x_i = 0.5$ for all i in Eqs. (21) and (22). This is the additional critical point whose existence was predicted on the basis of the state transition diagrams using topological arguments.

If Eqs. (21) and (22) are linearized at $x_i = 0.5$ (see Appendix), the characteristic equation is given by

$$\begin{vmatrix} -1 - p & -n/2 \\ \pm n/2 & -1 - p \end{vmatrix} = 0 \tag{23}$$

for $N = 2$, and is given by

$$\begin{vmatrix} -1 - p & 0 & -n/2 \\ \pm n/2 & -1 - p & 0 \\ 0 & n/2 & -1 - p \end{vmatrix} = 0 \, , \tag{24}$$

where the positive sign in the determinant is taken for Eq. (21) and the negative sign is taken for Eq. (22).

For Eq. (21) the eigenvalues are

$$p_{1,2} = -1 \pm ni/2 \tag{25}$$

for $N = 2$, and

$$p_1 = -1 - n/2 \, ,$$

$$p_{2,3} = -1 + n/4 \pm \sqrt{3} ni/4 \tag{26}$$

for $N = 3$. For all values of n (except $n = 4$), the critical point has an even number of positive real parts, confirming the topological predictions. The value $n = 4$, Eq. (26) is a *Hopf bifurcation* by definition, since at this value two of the eigenvalues cross the imaginary axis.[40,47,48] At the Hopf bifurcation, the critical point is not hyperbolic.

For Eq. (22) the eigenvalues are

$$p_{1,2} = -1 \pm n/2 \tag{27}$$

for $N = 2$, and

$$p_1 = -1 + n/2 \ ,$$
$$p_{2,3} = -1 - n/4 \pm \sqrt{3}ni/4 \tag{28}$$

for $N = 3$. From $n > 2$, this critical point has one eigenvalue with a positive real part, confirming again the topological predictions. If a detailed study of the dynamics is made, it is found that the two extremal steady states coalesce with the critical point at $x_i = 0.5$ for $n \leq 2$, as in Ref. 37. For the examples in this section, the topological predictions which are made for the critical point which are proven only in the limit $n \to \infty$, are in fact confirmed provided $n > 2$.

A large body of previous work can be conveniently classified into one of the classes just given on the basis of transitions between coarse grained volumes of concentration space found using Eq. (1). In performing the classification, we do not require that the differential equations for the system be written in the form given in Eq. (4). Kinetic equations displaying oscillation in two dimensions have been given for autocatalysis,[10,49–51] glycolysis,[52,53] mitosis,[54] predator–prey.[28,55] If the dynamics in all these systems is discretized by choosing the central focus for the thresholds for the two variables, all these equations fall in structure IV in Fig. 2. Oscillations in three dimensions have been found for the Field–Noyes equations,[14,15,22] and the feedback inhibition equations.[32,33,35,36,38] All these systems can be identified with structure XII', Table I. Bistability in two dimensions has been found in chemical systems with mutual activation,[37,56] mutual inhibition,[25,34,37,57] as well as in ecological systems with competitive exclusion[55] and lasers with mode competition.[58] By choosing the central saddle point as the threshold for the two variables, all these systems can be identified with structure I in Fig. 2.

VI. DISCUSSION

We have given a classification of chemical systems based on restrictions in the transitions between volumes of concentration space. Although for the systems in Eq. (4) there can only be transitions in one direction between adjacent volumes of phase space, in an arbitrarily complex chemical system there is no guarantee that such a restriction holds. However, the Hastings and Murray analysis[15,22] of the Field–Noyes equations,[14] which cannot be written in the form displayed in Eq. (3), indicates that there are, nevertheless, restrictions on transitions between volumes in this system of precisely the same sort found for Eq. (4). If it develops that transitions between adjacent volumes in concentration

space occur in one direction for a large class on nonlinear chemical systems, then the classification we have given will be of broad general interest.

Recent studies of nonlinear dynamics in ecological and chemical systems have provided a classification of hyperbolic critical points in terms of signs and locations of the nonzero terms in the matrix of the linearized equations at the steady state.[16,28,29] By embedding the dynamical system on a manifold and applying the Poincaré–Hopf theorem, we have extended this earlier work by giving restrictions on the entire set of critical points which are provided by the topological properties of the manifold. These restrictions are of particular interest in the analysis of complex systems, such as the bistable system in Eq. (22) in which there is more than one critical point. For any dynamical system with isolated hyperbolic critical points obeying the boundary conditions given in the Appendix, there must always be an odd number of critical points.

Our emphasis on classifying chemical networks by their qualitative dynamics can be contrasted with studies in which nonlinear chemical networks were classified on the basis of the structure of the mass action kinetic equations.[59] Although in both approaches similar mathematical techniques are used, the equivalence classes which are generated using the two approaches are very different. In the Horn analysis, 41 of 43 "isomorphism classes" which were enumerated in a recent study[59] had a single unique steady state. We have shown in Sec. IV that the continuous analogues of about half the structures generated in Table I must have multiple critical points.

We have used the Poincaré–Hopf theorem to aid in the location of critical points in Eq. (3), but it clearly can be used to give an enumeration of the various possibilities of the critical point structure for any chemical system. The major drawback of the Poincaré–Hopf theorem is that it gives *no* information about the dynamics in the remainder of phase space. It is therefore of some interest to study the dynamics of Eq. (4) in the limit as $t \to \infty$. There are at least three different behaviors in this limit.

(1) A trajectory can approach an extremal steady state defined in Eq. (11).

(2) A trajectory can oscillate in the region of a threshold of two or more variables. As it retraces its path through the same sequence of volumes, the amplitude of the oscillation decreases.

(3) A trajectory can reach a stable limit cycle oscillation. For $N = 3$, $n \to \infty$, one can prove there is a global limit cycle attractor in Eq. (21).[60]

It is likely that for any given structure, the qualitative dynamics remain invariant to changes in the parameters λ_i, γ_i, θ_i provided the inequalities $\lambda_i/\gamma_i > \theta_i$ are preserved.

In the preceding, all spatial factors have been completely ignored, and homogeneous reaction kinetics were assumed. However, heterogeneous catalysis and spatial localization can lead to a variety of interesting ef-

fects such as wave generation,[61] and dependence of the number and stability of critical points on the relative location of the localized catalysis.[37,62] Evidence has been given that there are global limit cycle oscillations in the simple feedback inhibition network with two chemicals if the synthetic sites are spatially separated but coupled by diffusive interactions.[37,40] Numerical evidence has been given that there can be both an extremal steady state and stable limit cycle oscillation in one of the equivalence classes given by structure XXXIV, Table I if the synthetic sites are spatially separated.[25,39]

The state transition diagrams can be computed directly from experimental data, by applying Eq. (1) with some appropriate choice of the θ_i. The classification scheme and the structure of the underlying network may thus provide a simple scheme for idealizing the qualitative dynamics and nonlinear interactions in complex chemical networks.

ACKNOWLEDGMENTS

APPENDIX: TOPOLOGICAL INDEX THEOREMS

We assume that there is a nonlinear dynamical system designated

$$\dot{\mathbf{x}} = f(\mathbf{x}) \ . \tag{A1}$$

A critical point of this system is any point for which $\dot{\mathbf{x}} = 0$. We assume that Eq. (A1) can be linearized in the neighborhood of $\mathbf{x}_{cp}$ and that the linearized equations are given by

$$\dot{\mathbf{x}} = A(\mathbf{x} - \mathbf{x}_{cp}) \ , \tag{A2}$$

where the elements of the matrix A are given by

$$a_{ij} = \frac{\partial f_i}{\partial x_j} \bigg|_{\mathbf{x}_{cp}} \ . \tag{A3}$$

The eigenvalues of the matrix designated p_i can be computed by solving the characteristic equation,

$$\det|A - pI| = 0 \ . \tag{A4}$$

If the $\mathrm{Re}\, p_i \neq 0$ for all i, $\mathbf{x}_{cp}$ is called a *hyperbolic critical point*. We assume that the dynamical system Eq. (A1) only has isolated hyperbolic critical points.[63]

The eigenvalues of the characteristic equation determine the *local* dynamics in the region of the critical point. For example, if $\mathrm{Re}\, p_i < 0$ for all i, the critical point is called *stable*, and all trajectories in the neighborhood of the critical point approach the critical point as $t \to \infty$. If $\mathrm{Re}\, p_i > 0$ for at least one i, the critical point is *unstable*. A classification of the hyperbolic critical points of two dimensional dynamical systems was given by Poincaré. The various cases were named as follows: focus, p_1 and p_2 are real complex conjugates; node, p_1 and p_2 are real with the same sign; saddle point, p_1 and p_2 are real with opposite signs. Foci and nodes can further be either stable or unstable. Saddle

points are always unstable.

But Poincaré went much further.[64] He proved a powerful and elegant theorem for dynamical systems embedded on two dimensional surfaces. He showed that

$$\mathfrak{N} + \mathfrak{F} - \mathfrak{S} = \chi(M) \ , \tag{A5}$$

where $\mathfrak{N}$, $\mathfrak{F}$, $\mathfrak{S}$ are the numbers of nodes, foci, and saddle points, respectively, of the dynamical system, and $\chi(M)$ is the Euler–Poincaré characteristic of the surface [$\chi(M)$ is 2 for a sphere, 0 for a torus, -2 for a torus with a handle, etc]. This theorem gives the interrelationships between the dynamics in different regions of phase space, and shows how they are connected to a topological invariant of the surface. The number and distribution of critical points in a dynamical system give information about the *global dynamics* in that system. Topological arguments have been used recently in the study of reaction mechanisms leading to oscillations in two dimensions.[51]

The generalization of Eq. (A5) to dynamical systems in arbitrary manifolds is called the Poincaré–Hopf theorem.[65] The *index* of a critical point is defined by

$$I = (-1)^{\mu_i} \ , \tag{A6}$$

where μ is the number of eigenvalues of a critical point for which $\mathrm{Re}\, p_i < 0$. The Poincaré–Hopf theorem is then

$$\sum_{cp} I = \chi(M) \ , \tag{A7}$$

where $\chi(M)$ is the Euler–Poincaré characteristic of the manifold.

As chemical kineticists, we are interested in a very simple manifold, the positive orthant of concentration space $x_i \geq 0$ for all i. Further, since the concentrations in any real chemical system are bounded, we can choose a sufficiently large concentration C such that $\dot{x}_i < 0$ for $|x| > C$. Since all chemical reactions are reversible, we further assume there will never be nonvanishing concentrations of any reagents, and that consequently all trajectories leave the axes $x_i = 0$ and enter the positive orthant. Our chemical phase space for N chemicals is therefore homeomorphic to a solid ball in N dimensions. Along the boundaries of the ball, trajectories only enter the ball. By identifying the boundary with a single point, a source at the south pole, the trajectories can be embedded on an N-sphere (the set of points $\sum_{i=1}^{N+1} x_i^2 = $ constant). The Euler–Poincaré characteristic for an N-sphere is given by[66]

$$\chi(M) = 1 + (-1)^N \ . \tag{A8}$$

Since there are no negative eigenvalues for the source at the south pole, its index is 1. Combining Eqs. (A6), (A7), (A8) gives

$$\sum (-1)^{\mu_i} = (-1)^N \ , \tag{A9}$$

where the sum is over all the critical points inside the ball in concentration space. If π_i is the number of positive eigenvalues at the ith critical point, we have $\mu_i + \pi_i = N$. Equation (A9) can then be rewritten

$$\sum (-1)^{r_i} = 1 \quad . \tag{A10}$$

In Sec. IV we show how this theorem can be used to deduce the existence of critical points for some of the structures in Fig. 2 and Table I.

In many equations which have been proposed to model chemical networks, a critical point falls on a boundary of the positive orthant so that $(x_i)_{c_p} = 0$ for some subset of the variables. The following mathematical test is proposed to determine whether these critical points on the boundary should be included in the summation in Eq. (A10). Consider all perturbations away from the boundary in the neighborhood of the critical points. If all trajectories return to the boundary, then the critical point must be included in the summation. For example, in Eq. (4) the extremal steady states which represent physically important critical points satisfy this test and must be included in the summation. If, however, all perturbations (except for a set of measure zero) do not return to the boundary, the critical point should not be included in the summation. For example, in the Field-Noyes equations[14] there is a critical point at the origin which is unstable. In applying the Poincaré–Hopf theorem to this system, this critical point must not be included. A justification for this exclusion comes from the observation that when the equations are mapped on the 3-sphere as described in the previous paragraph, this unstable critical point at the origin can be identified with the source at the south pole.

In Sec. III, a combinatorial version of Eq. (A5) was applied which is appropriate for directed graphs embedded on surfaces.[43] For each vertex and face of a directed graph, we define the number of *reversals* R at that vertex or face as follows. For a vertex, we examine each adjacent pair of edges terminating at the vertex. The number of adjacent pairs of edges at a vertex is equal to the number of edges terminating at a vertex. If both edges of an adjacent pair are either both directed towards, or away from, the vertex, the pair makes no contribution to the reversals at the vertex. Otherwise the pair makes a contribution of 1 to the reversals at the vertex. In a similar fashion, an adjacent pair of edges bounding a face makes no contribution to the reversals of the face if both edges are directed in a clockwise or counterclockwise orientation. Otherwise the pair makes a contribution of 1 to the reversals at the face. For each vertex and face, R is found by summing over all adjacent pairs of edges terminating at the vertex, or all adjacent pairs of edges bounding the face, respectively. R is always even. The index at each vertex and face is then

$$I = 1 - \tfrac{1}{2} R \quad , \tag{A11}$$

and the combinatorial index theorem is

$$\sum_{F, V} I = \chi(M) \quad , \tag{A12}$$

where $\chi(M)$ is the Euler–Poincaré characteristic of the surface on which the graph is embedded. The symbols in Eq. (5) give the only nonzero contributions to the index for the directed graph on the skeleton of the cube,

embedded on the sphere. In the text we refer to the symbols in Eq. (5) as stable nodes, unstable nodes, cycles, and saddles, respectively.

*Present address: Department of Physiology, McGill University, Montreal, Canada.
[1] R. E. Liesegang, Photo. Archiv. 21, 221 (1896); Naturw. Wschr. 11, 353 (1896).
[2] W. C. Bray, J. Am. Chem. Soc. 43, 1262 (1921).
[3] R. J. S. Rayleigh, Proc. R. Soc. A 99, 372 (1921).
[4] A. M. Turing, Philos. Trans. R. Soc. Lond. B 237, 37 (1952).
[5] J. Monod and F. Jacob, Cold Spring Harbor Symp. Quant. Biol. 25, 389 (1961).
[6] A. N. Zaikin and A. M. Zhabotinsky, Nature (Lond.) 225, 535 (1970).
[7] A. T. Winfree, Science 175, 634 (1972); 181, 137 (1973).
[8] J. A. DeSimone, D. L. Beil, and L. E. Scriven, Science 180, 946 (1973).
[9] *Biochemical Oscillators*, Proceedings of the 1968 Prague Symposium, edited by E. K. Pye and B. Chance (Academic, New York, 1973).
[10] P. Glansdorff and I. Prigogine, *Thermodynamics of Structure, Stability and Fluctuations* (Interscience, New York, 1971).
[11] G. Nicolis and J. Portnow, Chem. Rev. 73, 365 (1973).
[12] P. Ortoleva and J. Ross, Adv. Chem. Phys. (to be published).
[13] R. J. Field, E. Körös, and R. M. Noyes, J. Am. Chem. Soc. 94, 8649 (1972).
[14] R. J. Field and R. M. Noyes, J. Chem. Phys. 60, 1877 (1974).
[15] J. D. Murray, J. Chem. Phys. 61, 3610 (1974).
[16] J. J. Tyson, J. Chem. Phys. 62, 1010 (1975).
[17] B. L. Clark, J. Chem. Phys. 58, 5605 (1973); 60, 1481 (1974); 60, 1493 (1974).
[18] L. Van Hove, Phys. Rev. 89, 1189 (1953).
[19] J. C. Phillips, Phys. Rev. 104, 1263 (1956).
[20] J. C. Phillips and H. B. Rosenstock, J. Phys. Chem. Solids 5, 288 (1958).
[21] A. A. Maradudin, E. W. Montroll, G. H. Weiss, and I. P. Ipatova, *Theory of Lattice Dynamics in the Harmonic Approximation*, (Academic, New York, 1971), 2nd ed., Chap. 4.
[22] S. P. Hastings and J. D. Murray, SIAM J. Appl. Math (to be published).
[23] M. Sugita, J. Theor. Biol. 4, 179 (1963).
[24] S. A. Kauffman, *Lectures on Mathematics in the Life Sciences*, edited by M. Gerstenhaber (American Mathematical Society, Providence, RI, 1971), Vol. 3.
[25] L. Glass and S. A. Kauffman, J. Theor. Biol. 39, 103 (1973).
[26] R. Thomas, J. Theor. Biol. 42, 563 (1973).
[27] L. Glass, J. Theor. Biol. (to be published). This should be consulted for a fuller discussion of the combinatorial techniques which are used here. None of the topological results are contained in this earlier paper.
[28] R. M. May, *Stability and Complexity in Model Ecosystems* (Princeton U. P., Princeton, NJ, 1973).
[29] R. Levins, Ann. N.Y. Acad. Sci. 231, 123 (1974).
[30] F. Jacob and J. Monod, J. Mol. Biol. 3, 318 (1961).
[31] G. Yagil and E. Yagil, Biophys. J. 11, 11 (1971).
[32] B. Goodwin, *Temporal Organization in Cells* (Academic, London, 1963).
[33] M. Morales and D. McKay, Biophys. J. 7, 621 (1967).
[34] L. N. Grigorev, M. S. Polyakova, and D. S. Chernavskii, Mol. Biol. USSR 1, 349 (1967).
[35] C. F. Walter, J. Theor. Biol. 23, 39 (1969); 44, 219 (1974).
[36] J. S. Griffith, J. Theor. Biol. 20, 202, 209 (1968).
[37] R. M. Shymko and L. Glass, J. Chem. Phys. 60, 835 (1974).
[38] J. J. Tyson, J. Math. Biol. (to be published).
[39] L. Glass and S. A. Kauffman, J. Theor. Biol. 34, 219 (1972).
[40] L. Glass and R. Pérez, J. Chem. Phys. 61, 5242 (1974).

[41]In the limit $t \to \infty$, the maximum concentration for x_i is λ_i/γ_i. In all discussions which follow, we assume the concentrations are constrained to the box $0 \le x_i \le \lambda_i/\gamma_i$.

[42]M. A. Harrison, *Introduction to Switching and Automata Theory*, (McGraw-Hill, New York, 1965).

[43]L. Glass, J. Comb. Theory B 15, 264 (1973).

[44]Similar combinatorial and topological arguments have been used to classify directed graphs on the edges of an octahedron by the mathematician E. N. Gilbert in his paper, "The Ways to Build a Box," Mathematics Teacher (December 1971).

[45]S. W. Golomb, in *Information Theory, Fourth London Symposium*, edited by C. Cherry (Butterworths, London, 1961).

[46]J. Tyson, Third Colloquium for Automata Theory and Biological and Chemical Systems, Faculty de Medecine, Necker, Paris (to be published).

[47]N. Kopell and L. N. Howard, Studies Appl. Math. 52, 291 (1973).

[48]I. D. Hsü, J. Diff. Eqs. (to be published).

[49]I. Prigogine and R. Lefever, J. Chem. Phys. 48, 1695 (1968).

[50]J. Tyson, J. Chem. Phys. 58, 3919 (1973).

[51]J. J. Tyson and J. C. Light, J. Chem. Phys. 59, 4164 (1973).

[52]E. E. Sel'kov, Eur. J. Biochem. 4, 79 (1968).

[53]A. T. Winfree, Arch. Biochem. Biophys. 149, 388 (1972).

[54]J. Tyson and S. Kauffman, J. Math. Biol. (to be published).

[55]A. Rescigno and I. W. Richardson, in *Foundations of Mathematical Biology*, edited by R. Rosen, (Academic, New York, 1973), Vol. III.

[56]B. B. Edelstein, J. Theor. Biol. 37, 221 (1972).

[57]A. Babloyantz and G. Nicolis, J. Theor. Biol. 34, 185 (1972).

[58]W. Lamb, Phys. Rev. 134, A1429 (1964).

[59]F. Horn, Proc. R. Soc. Lond. A 334, 331 (1973).

[60]L. Glass (in preparation).

[61]P. Ortoleva and J. Ross, J. Chem. Phys. 58, 5673 (1973); 60, 5090 (1974).

[62]K. Bimpong-Rota, P. Ortoleva, and J. Ross, J. Chem. Phys. 60, 3124 (1974).

[63]A superb general reference with many interesting examples which has just appeared is M. W. Hirsch and S. Smale, *Differential Equations, Dynamical Systems, and Linear Algebra* (Academic, New York, 1974).

[64]H. Poincaré, *Oeuvres*, (Gauthier-Villars, Paris, (1928); Tome I. "Sur les courbes définies par les équations différentielles," Chap. XIII. Neophytes in the field who read French will appreciate Poincaré's no-nonsense approach to his famous theorem.

[65]Readers interested in greater detail should consult a text in differential topology. For example, the Poincaré–Hopf theorem, Eq. (A7), can be found in V. Guillemin and A. Pollack, *Differential Topology* (Prentice-Hall, Englewood Cliffs, NJ, 1974), p. 134. There is a very useful bibliography at the end of this text.

[66]For example, see Ref. 65, p. 131, problem 7.